

International Conference on Space Optics—ICSO 2008

Toulouse, France

14–17 October 2008

Edited by Josiane Costeraste, Errico Armandillo, and Nikos Karafolas



Quantum cascade lasers as metrological tools for space optics

S. Bartalini

S. Borri

I. Galli

D. Mazzotti

et al.



QUANTUM CASCADE LASERS AS METROLOGICAL TOOLS FOR SPACE OPTICS

S. Bartalini^{(1,2)*}, S. Borri^(1,2), I. Galli^(2,3), D. Mazzotti^(1,2), P. Cancio Pastor^(1,2), G. Giusfredi^(1,2), and P. De Natale^(1,2)

⁽¹⁾*Istituto Nazionale di Ottica Applicata (INOA) - CNR, IT-50125 Firenze, Italy, E-mail: saverio.bartalini@inoa.it*

⁽²⁾*European Laboratory for Non-Linear Spectroscopy (LENS), IT-50019 Sesto Fiorentino, Italy*

⁽³⁾*Dipartimento di Fisica, Università degli Studi di Firenze, IT-50019 Sesto Fiorentino, Italy*

ABSTRACT

A distributed-feedback quantum-cascade laser working in the 4.3–4.4 μm range has been frequency stabilized to the Lamb-dip center of a CO_2 ro-vibrational transition by means of first-derivative locking to the saturated absorption signal, and its absolute frequency counted with a kHz-level precision and an overall uncertainty of 75 kHz.

This has been made possible by an optical link between the QCL and a near-IR Optical Frequency Comb Synthesizer, thanks to a non-linear sum-frequency generation process with a fiber-amplified Nd:YAG laser. The implementation of a new spectroscopic technique, known as polarization spectroscopy, provides an improved signal for the locking loop, and will lead to a narrower laser emission and a drastic improvement in the frequency stability, that in principle is limited only by the stability of the optical frequency comb synthesizer (few parts in 10^{13}).

These results confirm quantum cascade lasers as reliable sources not only for high-sensitivity, but also for high-precision measurements, ranking them as optimal laser sources for space applications.

1. INTRODUCTION

Since their advent, Quantum Cascade Lasers (QCLs) have uniformly covered the mid and far infrared (IR), a region of the electromagnetic spectrum which has been ignored for a long time in many fields of applied physics, but which now is gaining more and more importance for a huge number of applications.

The areas of interest of this spectral region range from astrophysics to climatology, from trace gas detection in environmental monitoring to homeland security. For many of these applications, the migration to experiments in space represents a strategic improvement in terms of sensitivity and accuracy. For this reason the need of compact and reliable laser sources in the MIR and FIR region is even more compelling.

In our experimental work during last years we have demonstrated the versatility of QCLs in high sensitivity spectroscopic applications by implementing all the main frequency modulation techniques for sub-ppb detection of trace gases (N_2O , CH_4 and CO_2) [1].

In space applications QCLs can be used, for example, as local oscillators (LOs) in heterodyne spectrometry. They have represented an effective alternative in respect to CO_2 lasers, that have been for longtime the only sources allowing the sensitivity required by astrophysical applications. On the other hand, the finite number of frequencies covered by CO_2 lasers (including all the isotopomers) and the spectral range available (9–12 μm) were limiting the versatility of CO_2 laser based spectrometers. Different kinds of devices initially promising, such as lead salt diode lasers, have never provided significant improvements, mainly due to their insufficient power and their multi-mode behavior.

QC lasers recently used as LOs in mid-infrared heterodyne spectrometers [2,3], on the contrary, have proved to be able to replace CO_2 lasers in terms of emitted power, overcoming at the same time the limitations on the spectral range. At present, in fact, cw QC lasers working in the range from 3 μm to several tens of μm have been demonstrated [4,5,6].

A second aspect in which QCLs represent an important improvement in comparison to CO_2 lasers is the tunability. The typical tuning range of a single distributed-feedback (DFB) QC laser is 1–2 cm^{-1} , the tuning being induced by temperature or current variations. Based on this principle, micro-engineered stacks of QCLs working at adjacent wavelengths have been demonstrated, covering up to tens of cm^{-1} [7]. Even better performances have been recently obtained by using heterogeneous quantum cascade structures into an external cavity configuration [8]: single-mode tuning range of more than 100 cm^{-1} (10% the center wavelength) has been achieved.

On the side of spectral purity, upper limits to the emission linewidth of external cavity QCLs have been estimated in few MHz [9,10], and are the same order of magnitude of those measured for free-running DFB QCLs [11,12], also verified by our experiments [13]. This fact confirms that the external cavity does not significantly contribute to the narrowing of the emission linewidth. For a large number of applications these linewidths are well below the required resolution [2,3,14], but the possibility to have narrower sources (up to sub-kHz level) could path the way for a new generation of metrological space experiments.

A last aspect that has to be considered is the long-term

frequency stability, which can be assured only by an active stabilization of the laser sources, and is important in particular for the construction of secondary frequency standards in the mid-infrared.

In a very recent work [15] ultimate accuracies for the measurement of Doppler velocity drifts of 1 cm per second per year have been invoked, that are well beyond the performances of the actual spectrometers. Approaching to these levels, especially in the mid-IR region, will be of great importance for astronomical observation experiments.

The present manuscript describes our activity towards the development of simple and reliable techniques for the stabilization and the narrowing of the emission frequency of a cw QC laser. The lasers operates at 4.34 μm for temperatures below 100 K. An optical link to a near-IR optical frequency comb synthesizer (OFCS) through a sum-frequency generation (SFG) process allows a direct analysis of the emission spectrum and the absolute measurement of the frequency of the molecular transition the laser is locked to. The locking signal used in the first experiment is provided by a conventional first-derivative, wavelength modulation spectroscopy of a saturated-absorption Lamp-Dip feature.

In next section the cited results will be briefly presented, while in Sec.3 an alternative way of providing the locking signal, based on polarization spectroscopy, will be described. It will allow the locking to the transition center without any modulation of the laser frequency, with an enhanced bandwidth and with a simplification of the electronic.

2. FREQUENCY LOCKING OF A QCL AND ITS ABSOLUTE MEASUREMENT

This section offers an overview of the original experiment performed at LENS and described by the schematic setup of Fig.1. In the text the references to our previous works describing the details of the experiment will be found.

2.1 Optical link to a frequency COMB

The OFCS used in this experiment is a mode-locked femtosecond Ti:sapphire laser operating in the 500÷1100 nm range. In order to set a link between the OFCS and the QCL an up-conversion of its frequency is required. It has been achieved by a SFG process with a Nd:YAG laser into a non-linear periodically-poled LiNbO₃ crystal. The starting wavelengths are those of the QCL ($\lambda_{\text{QCL}} = 4.34 \mu\text{m}$) and of a Nd:YAG ($\lambda_{\text{YAG}} = 1.064 \mu\text{m}$), which is referenced to the OFCS. The obtained radiation, with a wavelength at about 854 nm, is superimposed to the beam of a laser diode working at

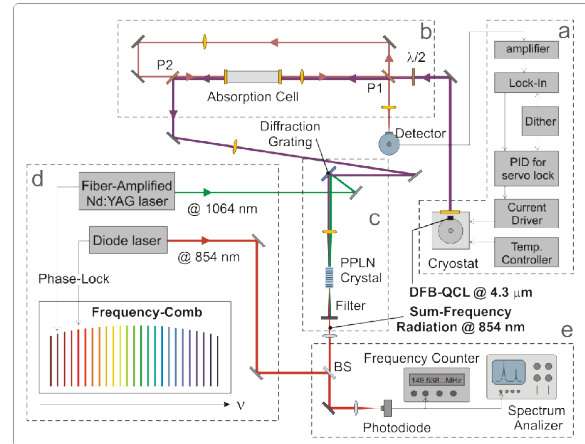


Fig.1. Schematic setup describing the main parts of the experiment: a) QCL housed in its cryostat and electronics; b) Saturated absorption spectroscopy; c) Sum-frequency generation in PPLN crystal; d) OFCS and OFCS-referenced lasers; e) Beat-note detection, frequency analysis and counting.

a close wavelength and referenced to the OFCS too. A fast photodiode detects the radio-frequency beat-note, the signal is analyzed by a spectrum analyzer and its frequency measured by a counter. The details of the experimental setup and of the direct digital synthesis (DDS) method used for referencing the Nd:YAG and the laser diode to the OFCS are reported in [13,16,17,18]. The important point is that the locking scheme used makes the beat note spectrum to exactly reproduce the line-shape of the QCL emission spectrum, and from the counting of its frequency (ν_{beat}) it is possible to derive the absolute value of the QCL frequency by:

$$\nu_{\text{QCL}} = \nu_{\text{diode}} - \nu_{\text{YAG}} + \nu_{\text{beat}}, \quad (1)$$

since ν_{YAG} e ν_{diode} are known with the OFCS precision and have few-kHz-linewidths, negligible in comparison with the QC laser linewidth.

2.2 Sub-Doppler FM Spectroscopy and frequency locking

Unlike other experimental works [19,20], where the QCL frequency has been locked even at very high levels, but without any absolute reference, our aim was to use, for frequency stabilization, the narrowest feature having also absolute reference and intrinsic stability characteristics. We opted for the Lamb-Dip of a molecular CO₂ line, obtained by a typical saturated absorption spectroscopy setup, described in details in [13]. Even considering the pressure and transit time broadening effects, determined by our experimental conditions, the total width of the Lamb-Dip feature is not larger than 200 kHz.

The dispersive signal centered on the line has been obtained by a conventional wavelength modulation of

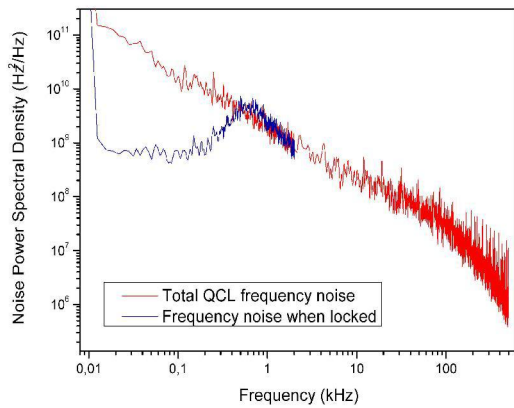


Fig.2. Comparison between the laser frequency noise in free-running (red) and locking (blue) conditions. The bandwidth below 1 kHz is what we expected considering the 1 ms lock-in time constant.

the laser and a lock-in first-derivative detection of the absorption signal. This feedback signal is processed by a PID and then sent to the laser, together with the dither, through the modulation input of the low-noise current driver.

In our case, the bandwidth of the feed-back signal is limited by the 1 ms time constant of the lock-in; in general, the critical point is the presence of the dither itself, since it occupies most of the available modulation bandwidth at the expense of the feed-back signal bandwidth, the only playing a role in frequency stabilization. Our current driver, for example, has a 150 kHz modulation bandwidth, and the feed-back signal bandwidth could not be anyway larger than few tens of kHz. This value is still not enough for a linewidth narrowing, as we will see in the following.

In principle it is possible to send the dither signal directly to the QCL bypassing the current driver and avoiding the limitations imposed by its bandwidth, but it is a dangerous choice, since the device is very sensitive to electrical shocks and the risk of breaking it was too high.

We do not report here the graphs with the saturated absorption signal and its first-derivative. They are shown in Sec.3 where a comparison with the polarization spectroscopy is presented.

A clear representation of the effectiveness of the locking loop is provided by the comparison between the frequency noise spectra in free-running and locking conditions, shown in Fig.2. Both spectra have been acquired by using the slope of the transmission peak of a germanium etalon as a frequency-to-amplitude-noise discriminator. The small loop bandwidth is determined, as already stated, by the lock-in 1 ms time constant; the noise suppression of up to 25 dBm is satisfying and ensures a good long-term stability of the frequency, as described in the following.

2.3 QCL emission lineshape analysis and absolute frequency and stability measurement

From the analysis of the beat-note spectrum we can directly characterize the QCL frequency noise, obtaining informations that are complementary to those of Fig.2. The real-time FFT spectrum analyzer allows to follow the time evolution of the beat-note spectrum with a resolution of 40 μ s, corresponding to the frame rate of the FFT spectra (25 kHz).

Fig.3(a) shows the time evolution of the beat-note during a 2 ms interval, with the free-running QCL; an acquisition over longer timescales was not possible because the fluctuations were larger than the maximum available frequency span of the analyzer (only 15 MHz in real-time mode). Such fluctuations, as well as the width of the fast jittering envelope, heavily depend on the current noise of the driver. This is clearly shown by a comparison with Fig.3(b), in which the same QCL is powered by an ultra low-noise home made driver: not only the peak is sharper, but also its fluctuations are smaller, and it is possible to follow the evolution for a longer time (10 ms). Unfortunately, the home made current driver is still not provided by a modulation input, and it is not yet suitable for frequency locking.

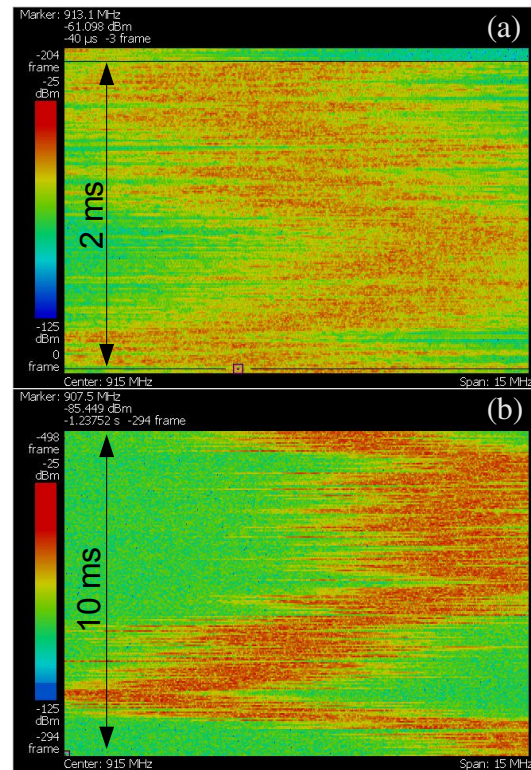


Fig.3. The evolution of the beat note as detected by our real-time spectrum analyzer, with the QCL powered by a commercial low-noise driver (a) and by a home-made ultra low-noise driver (b). Different current noise levels determine different fluctuation amplitudes of the QCL frequency.

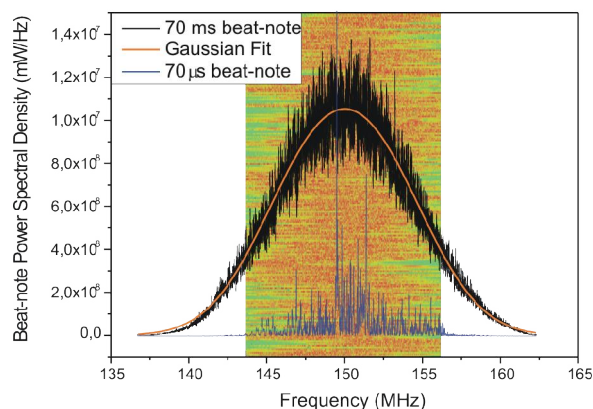


Fig. 4. The blue profile is the FFT spectrum of a 40 μ s-long acquisition of the beat-note, while the black one is the FFT of a 70 ms-long acquisition. The latter can be interpreted also as an average of 1750 spectra of the blue type. In background a 10 ms-long real-time acquisition during locking is shown. The maximum frequency span in single FFT mode is double than in real-time mode.

The effects of the locking loop can be analyzed by observing the beat-note spectrum with the loop on: in this condition the fluctuations are reduced, and lie well within the analyzer spectral window, so that longer acquisitions are possible. Fig.4 shows a comparison between two spectra corresponding to 70 ms and 40 ms acquisition lengths, both with the laser locked: the intrinsic linewidth appears very narrow but, even in locked condition, the non suppressed fast jitter determines a gaussian broadening of the line shape over long timescales.

Anyway, the regular shape of this gaussian envelope, ensured by the locking, allows an affordable frequency counting. In fact, the frequency counter used has a 1 s gate time, thus averaging all the faster random jitter and achieving a short-term precision drastically better than the linewidth of the laser.

Fig.5 shows a comparison between two typical sets of frequency counts, with the QCL in free-running and locked operation. The stability achieved by the locking enables the acquisition of several hundreds of points, and allows to minimize the statistical error. In this way a standard deviation, on a single data set, of a few kHz can be achieved. This can be assumed as the intrinsic precision of our system. Unfortunately the presence of unwanted slow drifts ascribed, for example, to interference fringes shifting the locking point, limits the overall accuracy to the level of some tens of kHz. However, the final precision of the measurement of the molecular transition absolute frequency is about two orders of magnitude better than the error stated by the HITRAN database.

The next step is an improvement of the loop bandwidth and gain, in order to achieve a narrowing of the laser emission, together with an enhancement of the stability

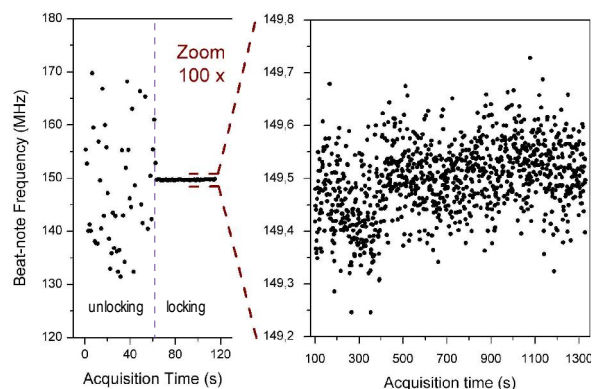


Fig. 5. The frequency locking loop reduces the spread of the frequency counts by a factor comparable to its gain (>20 dB). An example of a 20 minutes-long data set is shown in the right part of the graph.

of the error signal, in order to eliminate the spurious effects that limit the final precision.

3. MID INFRARED SUB-DOPPLER POLARIZATION SPECTROSCOPY

We believe that, together with the development of current drivers with better noise performances and higher modulation bandwidths, the new approach of polarization spectroscopy will be an important milestone towards the solution of the problems cited above. In the following the advances in this direction will be presented.

3.1 Principle and advantages

Polarization spectroscopy is among the most sensitive spectroscopic techniques [21,22], even if it is still not widely used. It is a pump-probe technique like the saturation spectroscopy, and it is based on the detection of an optical anisotropy induced in a medium by the pump beam. It works for every ro-vibrational molecular transition, and thus it has a very wide range of applicability in the mid-infrared region, that is precisely known as the molecular fingerprint region, thanks to the presence of the most intense ro-vibrational bands of many common molecules.

Its principle is to induce a birefringence in a medium, with a circularly polarized pump beam, and to interrogate this with a linearly polarized counterpropagating probe beam, watching for the rotation of its polarization. It can be regarded as a form of saturation spectroscopy, with the change of the complex refractive index being proportional to the pump intensity.

To our knowledge, the results presented here are the first reporting the successful utilization of this technique in the mid-IR region and with a QC laser.

As we have already stated, it offers several chances of improving our experiment.

The key concept is the production of a dispersive signal suitable for frequency locking without any modulation (dither) on the driver current.

The absence of the dither offers a direct benefit from the point of view of spectral purity. Moreover it allows a complete exploitation of the modulation bandwidth available for the locking loop, and thus for frequency noise reduction. Moreover, it simplifies the electronics involved in the locking loop (the lock-in is no more required), and this is a valuable point in the perspective of a space-oriented experiment.

Also from the point of view of sensitivity, polarization spectroscopy is an important advance, and will enhance the loop gain by improving the signal-to-noise ratio.

The limitations of this technique involve especially the single detection scheme, presented in the following. In fact it does not provide a zero background signal, the locking point can not be easily determined and is affected by offset variations, at the expense of the stability. As we will see, it is possible to overcome these restrictions by adopting a double detector differential acquisition setup, that we are going to implement soon.

3.2 Experimental Set-Up and test acquisitions

The changes made in the experimental set-up have involved only the manipulation of the beams polarizations, as shown in Fig.6. The tunable $\lambda/2$ waveplate, in combination with first wire grid polarizer (P1), splits the QCL beam into the pump and probe beams. The polarization of the former is set to circular by the tunable $\lambda/4$ waveplate. The polarization of the probe beam is already linear since it is determined by the first polarizer, but it is further cleaned by the P2 polarizer, just before the spectroscopy cell. After the cell the probe beam encounters the analysis polarizer (P3) and its transmitted component is detected.

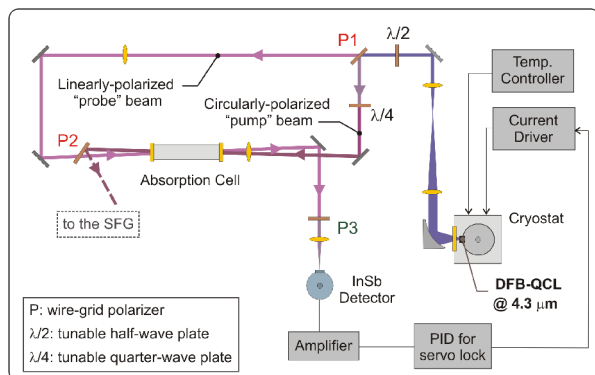


Fig.6. Schematic of the polarization spectroscopy setup. The polarizers P1 and P2 are parallel; P3, the analysis polarizer, is nearly crossed in respect to the others. The electronic apparatus required for locking is drastically simplified with respect to Fig. 1.

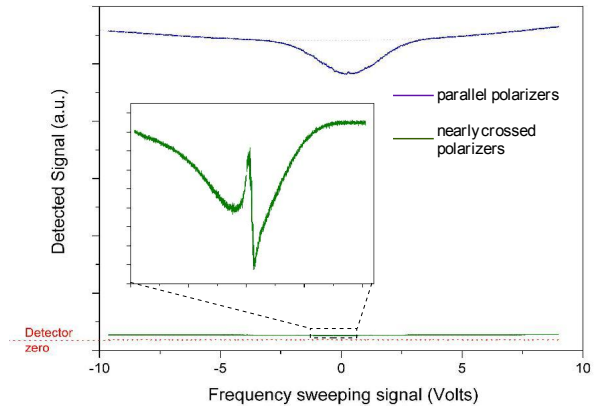


Fig.7. By tuning the orientation of the analysis polarizer it is possible to continuously move from the usual saturated absorption signal to the polarization spectroscopy signal. The polarization signal is intrinsically weaker since it is obtained for nearly crossed polarizers.

In this first experiment the polarizers P2 and P3 are nearly crossed: this means that the detected signal is very weak, compared with the typical amplitude of a saturated absorption signal (Fig.7). For this reason a larger amplification has been applied to the detected signal.

The dispersive profile appears in place of the Lamb-Dip, or better overlapped to it, since the background sub-Doppler profile is still present, and grows faster when moving far from the nearly crossed position. On the other hand, for perfectly crossed polarizers, no dispersion signal is present. Due to the residual background, the signal is not symmetric and suffers from offset fluctuations. A test of frequency locking performed with this signal did not lead to significant improvements in respect to the first-derivative locking loop, mainly because of amplitude fluctuations of the error signal itself.

However the improvements made in terms of sensitivity and bandwidth of the signal are noticeable. Fig.8(a) shows a comparison between a simple saturated absorption signal and the polarization signal: a S/N enhancement of more than a factor 5 is achieved without any effective bandwidth reduction. On the other hand, Fig.8(b) points out the improvement, in terms of bandwidth, in comparison with the first-derivative dither-locking technique. In fact it is evident how, in that case, a comparable signal-to-noise ratio is obtained at the expenses of a smaller signal bandwidth. The comparison between the slopes is a further evidence of this fact.

It has to be pointed out that here the factor limiting the steepness of the slope is the laser emission linewidth: with a better current driver we plan to see even sharper features with the polarization spectroscopy, where with first-derivative spectroscopy the presence of the modulation and the lock-in time constant would have prevented a better resolution.

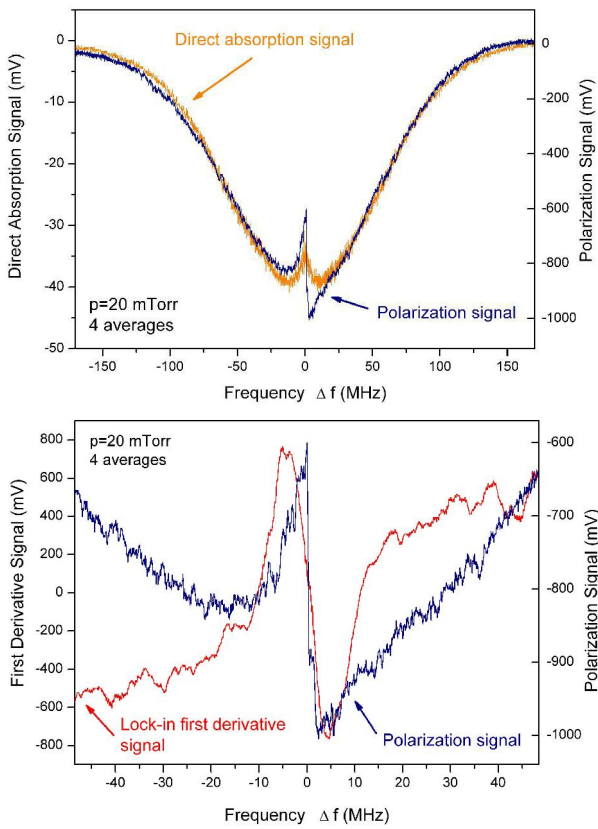


Fig.8. (a) Comparison between the direct saturated-absorption signal and the polarization spectroscopy signal. Both are obtained without any dither on the driver current. (b) Comparison between the sub-Doppler feature acquired in first-derivative lock-in mode and in polarization spectroscopy mode. The signal bandwidth is larger in the second case, thanks to the absence of the dither.

3.3 Double-detector polarization spectroscopy

With the double-detection differential polarization spectroscopy the analysis wire-grid polarizer is rotated by 45° in respect to its original position, and both the transmitted and reflected components are detected. In this way the polarization effect is equally split into the two channels, with opposite sign, as well as the common background, but with the same sign. The differential acquisition thus allows to cut off the background contribution, together with the related amplitude fluctuations. At the same time, the polarization signal is enhanced and assumes a symmetric shape centered on the line, ideal for the locking signal.

Even if we still have not implemented the upgrade to double-detection polarization spectroscopy, we can simulate the expected signal. First of all we have checked if the theoretical model presented in [22] is able to reproduce the signals acquired in single detection polarization spectroscopy. This has been successfully verified, and Fig.9 shows the good

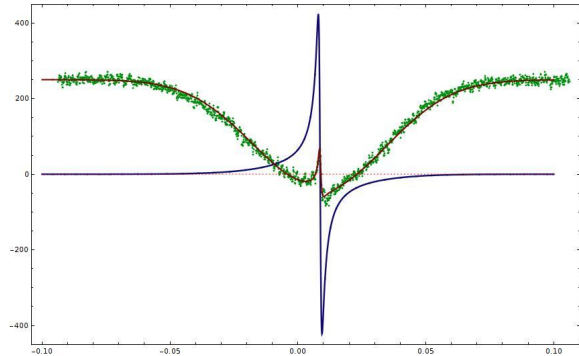


Fig.9. The simulation (dark red line) describes very well the experimental data acquired in single detection mode (green points) and permits to reconstruct the signal expected in the same experimental conditions by switching to the differential detection mode (blue line).

agreement between an experimental profile and its fit performed with the model equation. At this point it is possible to conveniently modify the parameters in order to reproduce the differential acquisition signal expected in the same experimental conditions. The result is shown in the same Fig.9 and is consistent with the expectations: the signal is enhanced, perfectly symmetric and with no background. We intend to use this signal for our next frequency locking loop, and we expect significant improvements on all the critical aspects: bandwidth, gain, sensitivity and stability.

4. CONCLUSIONS

In this work we summarize our activity oriented to the stabilization of the frequency of a mid-IR QC laser to a molecular ro-vibrational transition. The characterization of the locking loop is made possible by an optical link to an OFCS, that enables absolute measurements of the molecular transition frequency with a relative short-term precision of 5 parts in 10^{11} (3.5 kHz) and an overall uncertainty of 75 kHz limited by systematics.

A new approach based on polarization spectroscopy has been implemented in order to overcome many of the limitations occurred with the previous first-derivative dither-locking technique.

Thanks to these advances we plan to achieve, in the stabilization of the QC laser frequency to the center of a sub-Doppler molecular Lamb-Dip, the same performances already obtained by other groups in the stabilization of similar devices to cavities or to Doppler-broadened spectroscopic features. This will soon make possible to design secondary frequency standards for a huge number of wavelengths in the mid-IR region. These QCL-based sources will have several mW power, kHz emission linewidths and excellent long-term stability, and will be suitable for high resolution heterodyne spectrometers, space communications and metrological experiments in space.

5. REFERENCES

1. Borri S., et al. Frequency modulation spectroscopy by means of quantum-cascade lasers, *Appl. Phys. B* 85, 223–229, 2006.
2. Parvite B., et al. Preliminary results of heterodyne detection with quantum-cascade lasers in the 9 μm region, *Spectr. Acta A* 60, 3285-3290, 2004.
3. Sonnabend G., et al. Observations of Martian non-thermal CO_2 emission near 10 μm with a new tuneable heterodyne receiver, *Astron. Astrophys.* 435, 1181–1184, 2005.
4. Devenson J., et al. Very short wavelength ($\lambda = 3.1\text{-}3.3$ μm) quantum cascade lasers, *Appl. Phys. Lett.* 89, 191115, 2006.
5. Revin D., et al. InGaAs/AlAsSb/InP quantum cascade lasers operating at wavelengths close to 3 μm , *Appl. Phys. Lett.* 90, 021108, 2007.
6. Fan J., et al. Wide-ridge metal-metal terahertz quantum cascade lasers with high-order lateral mode suppression, *Appl. Phys. Lett.* 92, 031106, 2008.
7. Lee B., et al. Widely tunable single-mode quantum cascade laser source for mid-infrared spectroscopy, *Appl. Phys. Lett.* 91, 231101, 2007.
8. Maulini R., et al. External cavity quantum-cascade laser tunable from 8.2 to 10.4 μm using a gain element with a heterogeneous cascade, *Appl. Phys. Lett.* 88, 201113, 2006.
9. Maulini R., et al. Continuous-wave operation of a broadly tunable thermoelectrically cooled external cavity quantum-cascade laser, *Opt. Lett.* 30, 2584-2586, 2005.
10. Sonnabend G., et al. Evaluation of quantum-cascade lasers as local oscillators for infrared heterodyne spectroscopy, *Appl. Opt.* 44, 7170-7172, 2005.
11. Ganser H., et al. Investigation of the spectral width of quantum cascade laser emission near 5.2 μm by a heterodyne experiment, *Opt. Commun.* 197, 127–130, 2001.
12. Weidmann D., et al. Free-running 9.1 μm distributed-feedback quantum cascade laser linewidth measurement by heterodyning with a CO_2 laser, *Opt. Lett.* 28, 704–706, 2003.
13. Borri S., et al. Lamb-dip-locked quantum cascade laser for comb-referenced IR absolute frequency measurements, *Opt. Express* 16, 11637, 2008.
14. Krötz P., et al. Applications for quantum cascade lasers and detectors in mid-infrared high-resolution heterodyne astronomy, *Appl. Phys. B* 90, 187–190, 2008.
15. Steinmetz T., et al. Laser Frequency Combs for Astronomical Observations, *Science* 321, 1335, 2008.
16. Bartalini S., et al. Frequency-comb-referenced quantum-cascade laser at 4.4 μm , *Opt. Letters* 32, 988, 2007.
17. Stenger J., et al. Ultraprecise Measurement of Optical Frequency Ratios, *Phys. Rev. Lett.* 88, 073601, 2002.
18. Telle H. R., et al. Kerr-lens mode-locked lasers as transfer oscillators for optical frequency measurements, *Appl. Phys. B* 74, 1–6, 2002.
19. Williams R., et al. Kilohertz linewidth from frequency-stabilized mid-infrared quantum cascade lasers, *Opt. Lett.* 24, 1844-1846, 1999.
20. Taubman M. S., et al., Frequency stabilization of quantum-cascade lasers by use of optical cavities, *Opt. Lett.* 27, 2164-2166, 2002.
21. Wieman C. and Hänsch T. W., Doppler Free Laser Polarization Spectroscopy, *Phys. Rev. Lett.* 36, 1170-1173, 1976.
22. Demtröder W., *Laser Spectroscopy 2nd edition*, Springer, Berlin, 454-466, 1973.